Photoelectron spectroscopy without photoelectrons: Twenty years of ZEKE spectroscopy

Martin C. R. Cockett

Received 18th July 2005
First published as an Advance Article on the web 5th September 2005
DOI: 10.1039/b505794a

Zero Kinetic Energy (ZEKE) spectroscopy, originally developed as a high resolution form of photoelectron spectroscopy, promised a means to the unambiguous determination of ionic (ro)vibrational states. Since its original development, it has spawned numerous methodological offshoots and has become one of the default methods of choice for high resolution spectroscopy of the ion. This *tutorial review* describes the historical development of the method, provides some insight into how it works and assesses the impact of the technique by reviewing some of the highlights of the past 20 years as well as some of the more recent developments and applications.

Introduction

A little over twenty years ago the first papers were published[1] detailing the development of a new form of photoelectron spectroscopy, which claimed to offer laser bandwidth limited spectral resolution. The method was termed at the time photo-ionisation resonance spectroscopy (PIRS) and was based on the principle that detection of zero kinetic energy photoelectrons produced at resonances in the ionisation continuum provided unambiguous determination of ionic (ro)vibrational states. The method is now better known as zero kinetic energy (ZEKE) spectroscopy and its development has seen an explosion of activity in high resolution spectroscopy of the ion. It has also spawned a number of new techniques based on the same principles as well as a wide range of applications outside high resolution ionic spectroscopy which could not have been foreseen at the time of its original development. This article aims to assess the impact of the technique by reviewing some of the highlights of the past 20 years as well as some of the more recent developments and applications.

Department of Chemistry, University of York, Heslington, York, UK YO24 4AA. E-mail: mcrc1@york.ac.uk; Fax: 01904 432516; Tel: 01904 434534

Martin Cockett

Martin Cockett is a senior lecturer in the Department of Chemistry at the University of York. He graduated in 1986 from the University of Sussex with a BSc Hons in Chemical Physics before moving to Southampton University where he studied for his PhD in free radical photoelectron spectroscopy under Professor John Dyke. Following his PhD he spent two years in Japan as a JSPS/Royal Society post-doctoral fellow at the Institute for Molecular Science, working in the laboratory of Professor Katsumi Kimura on the application of ZEKE spectroscopy to the study of aromatic van der Waals complexes. Following a further three years in the Department of Chemistry at the University of Edinburgh, initially as a postdoctoral fellow and then as a lecturer, he extended his interest in weak interactions to Rydberg and ionic states of small inorganic van der Waals complexes and applied ZEKE spectroscopy to the study of electronically excited states of small molecular ions. In 1996 he was appointed to a lectureship at the University of York where his research has focused on non-covalent interactions, Rydberg state dynamics and more recently, ion-molecule reactions in clusters.

Background

The development of UV photoelectron spectroscopy in the early 1960's by Turner[2] and Vilesov[3] provided the only experimental means to validate the concept of the molecular orbital as conceived by Mulliken.[4] The original idea involved photo-ionisation of a gas phase sample using fixed wavelength radiation, typically provided by a HeI discharge lamp. The photoelectrons emerge from the encounter with a distribution of kinetic energies which depend on the energy of the ionising radiation and the final state of the ion. The connection between a photoelectron spectrum and the molecular orbital energies is provided by Koopmans' theorem[5] which states that the ionisation energy of a particular photoelectron band is equal to the negative of the orbital energy of the orbital from which the electron originated. Consequently, a photoelectron spectrum can be regarded as a map of the molecular orbitals in a molecule. The correlation with MO energies is founded on some fundamental approximations which hold true frequently enough for Koopmans' theorem to hold water, but breaks down completely for ionisation from open shell molecules and for molecules where the molecular orbital ordering changes in the cation. Whilst the molecular orbital view of photoelectron spectroscopy holds tremendous appeal, it is perhaps more appropriate to view the photo-ionisation process as an electronic transition between the ground state of the neutral molecule and a particular electronic state of the cation: the photoelectron spectrum then provides an unambiguous view of

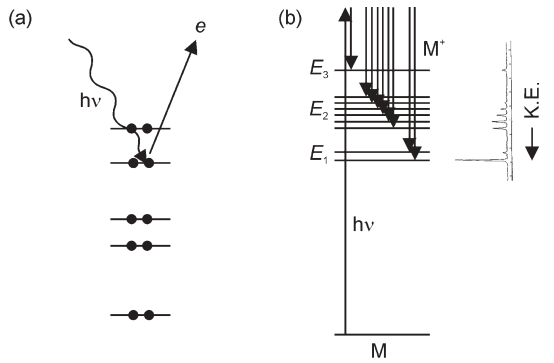

Fig. 1 Photo-ionisation can be represented alternatively as (a) ejection of an electron from an atomic or molecular orbital or (b) an electronic transition between the neutral ground state (represented by M in the Figure) and various electronically excited states of the cation (E_1, E_2 and E_3). For a given photon energy, the more highly excited the cation, the lower the kinetic energy (K.E.) of the photoelectrons.

the electronic states of the cation whilst still providing information about the character of the molecular orbitals of the neutral molecule through the observation and extent of vibrational fine structure. The two representations of the ionisation process are shown in Fig. 1.

In spite of the enormous diversity of applications to which photoelectron spectroscopy has been applied in both the condensed and gas phases, it is now less commonly used as a pure spectroscopic technique for gas phase valence studies of molecules because the spectral resolution is typically poor compared to that achievable in other areas of gas phase electronic spectroscopy. This is because the key requirement to measure the electron kinetic energy typically limits the working resolution to about 10 meV (80 cm^{-1}). Historically, two alternative approaches have been adopted to overcome this shortcoming: The first retains the basic premise that ionisation is achieved by fixed energy photon sources but aims to improve the precision with which the electron kinetic energy is measured. One major step towards achieving this came in the early 1980's with the application of laser multiphoton ionisation techniques coupled to time-of-flight kinetic energy analysis. This allowed not only the minimisation of excess energy required to achieve the best energy resolution but also the advantages of state selection and very narrow bandwidth radiation. Further improvements in resolution were achieved through the use of magnetic bottle electron energy analysers[6] but the most spectacular advance has come very recently from a very careful application of the principles detailed above but with special attention paid to the reduction of point charges in the ionisation region. In these experiments, Weinkauf *et al.*[7] achieved resolution of between 0.5 and 1 meV (4–8 cm^{-1}) in their time-of-flight REMPI-PE spectra of n-propylbenzene. However, regardless of the route chosen to achieve better kinetic energy analysis of the photoelectrons, the method remains very sensitive to the type of sample being studied, with the very best resolution not easily achievable with anything other than relatively inert samples.

The second approach turns the whole concept on its head by simply dispensing with electron kinetic energy analysis and instead collecting threshold photoelectrons (TPE) produced as a tuneable light source is scanned through successive ionisation thresholds (see Fig. 2). Photoelectrons produced at each threshold, by definition, have close to zero kinetic energy and their yield increases dramatically when the photon source is on-resonance. The resulting spectrum thus provides a map of the ionisation thresholds as a function of wavelength. The beauty of this concept is that, assuming sufficiently good discrimination between electrons produced at a particular ionisation threshold and photoelectrons correlated with lower thresholds (*i.e.* those having some kinetic energy), the resolution of the method is simply limited by the bandwidth of the radiation used to achieve ionisation. The first implementations of this idea can be traced back to the late 1960's in the early experiments of Villarejo and co-workers who employed a differential electron-energy analyzer to detect photoelectrons produced with nearly zero initial kinetic energy as a function of photon energy.[8] Using dispersed Hopfield continuum radiation from a 1 m monochrometer, they achieved a resolution comparable to the radiation bandwidth of 50 meV. Some improvements in resolution were achieved in the so-called Photo-ionisation Resonance Spectra of Peatman *et al.*[9] who exploited the steradiancy properties of the ionisation source to detect true zero kinetic energy electrons. Coupled to a high pressure argon continuum source with a vacuum UV monochrometer they achieved a resolution of 33 meV in their spectra of NO, although the electron analyser was subsequently shown to be capable of resolving better than 1 meV. In terms of working resolution these approaches were not demonstrably superior at the time of their introduction to conventional fixed wavelength photoelectron spectroscopy, but they did demonstrate the enormous potential of the method. Modern incarnations of this approach are generally known as threshold photoelectron spectroscopy (TPES) and typically employ synchrotron radiation which, when combined with penetrating field electron analysers can provide resolution as low as 1 meV but more typically in the 5 to 10 meV range.[10] Whilst the efficacy of this approach has been demonstrated by

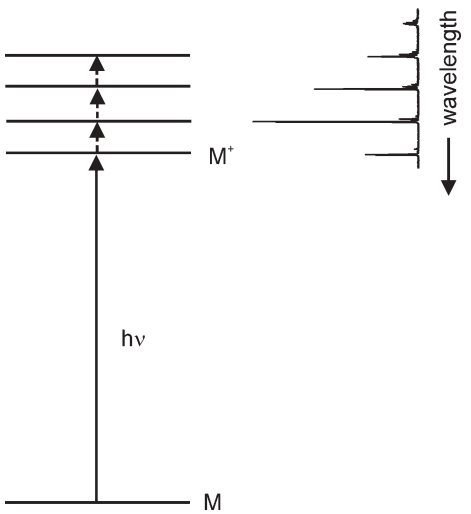

Fig. 2 In threshold photoelectron spectroscopy, the spectrum is obtained by collecting threshold photoelectrons (those with little or no kinetic energy) that are produced as a tuneable source of ionising radiation is scanned across each ionisation threshold.

its longevity and the wide range of experimental techniques that it has spawned, its application to high resolution spectroscopy had to wait for the widespread commercial availability of tuneable lasers with their associated very narrow bandwidths.

Zero kinetic energy spectroscopy

In 1984 the first papers appeared reporting the development of a novel method capable of resolving rotational ionic states by detection of threshold electrons.[1] The method combined supersonic free jet expansion techniques with laser multi-photon ionisation and pulsed electric field discrimination and achieved a resolution of 1.2 cm^{-1} in resolving the first three rotational states of NO^+. The success of the approach reported in these papers was based on the principle that electrons with zero kinetic energy can be distinguished from those with kinetic energy by imposing a delay between the ionisation event (correlated with a laser pulse) and the subsequent application of a pulsed electric field. Assuming that electrons with kinetic energy move, and those without do not, following ionisation, the kinetic electrons will be separated spatially from the ZEKE electrons by an amount which depends on their kinetic energy and the length of time that passes. Provided suitable acceleration and drift regions are used in the apparatus, the different groups of electrons can, in principle, be separated according to their time-of-flight to a detector (see Fig. 3). This premise requires that the zero kinetic energy

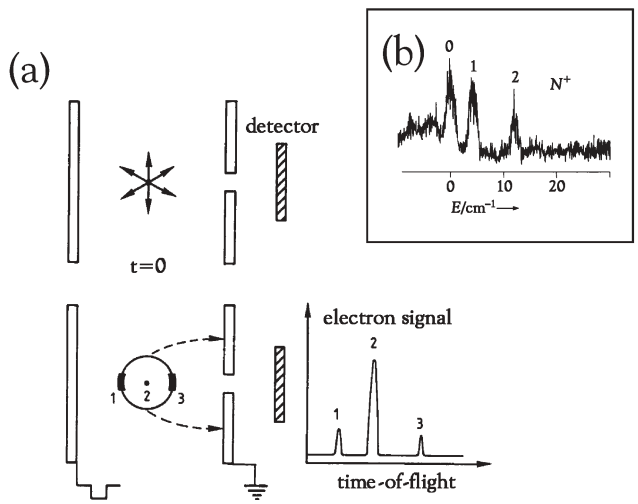

Fig. 3 (a) A schematic representation of the ionisation process in ZEKE spectroscopy. At $t = 0$, a laser pulse tuned to some ionisation threshold generates a mixture of threshold electrons (of nominally zero kinetic energy) and fast photoelectrons. After a suitable delay, the fast electrons will have moved away from the ionisation point allowing temporal discrimination between ZEKE electrons and fast electrons by their respective times-of-flight to a detector. (b) The first ZEKE spectrum, showing the first three rotational levels of NO^+. [Reprinted with permission from (a) K. Müller-Dethlefs, *Applications of ZEKE Spectroscopy*, ref. 46, Copyright 1995 Elsevier. (b) (modified from) K. Müller-Dethlefs, M. Sander and E.W. Schlag, *Two-Colour Photoionization Resonance Spectroscopy of NO: Complete Separation of Rotational Levels of NO^+ at the Ionization Threshold*, ref. 1, Copyright 1984 Elsevier.]

electrons are prepared in as close to a zero field environment as possible in order to minimise any field induced drift of the electrons away from the ionisation point. Just how difficult this is to achieve did not become apparent until 1988 when it was noted that the ionisation energy of NO obtained from ZEKE spectroscopy was lower than that obtained from Rydberg extrapolation.[11] Furthermore, the magnitude of this red-shift in ionisation energy was found to depend directly on the electric field strength used to accelerate the electrons towards the detector and it was this observation that lead to the realisation that the signal observed in a ZEKE experiment derives not from zero kinetic energy photoelectrons but from the field ionisation of very highly excited electronic states lying just beneath each threshold (see Fig. 4). These states, known as Rydberg states, are electronic states characterised by principal quantum numbers, n, larger than that which describes the valence shell. Rydberg states lying just beneath each ionisation threshold will have very large values of n and, because the size of the electron orbit scales with n^2, will have very large orbits which, in principle, render them less sensitive to decay processes. However, high-n Rydberg character alone is not sufficient to allow the states to survive the typical delays employed in the ZEKE experiments (ranging from a few hundred nanoseconds to several microseconds) – they must somehow acquire additional character which limits the options available to the Rydberg state for decay.

ZEKE Rydberg state lifetimes

One of the real surprises to many of the early adopters of the ZEKE method was the robustness and longevity of the Rydberg states sampled in a typical ZEKE experiment. This surprise was born from the expectation that Rydberg states populated by the optical transition from the initial state (typically the first valence excited state of the molecule, or less typically the electronic ground state) are likely to be of low orbital angular momentum ($\ell \leqslant 2$) character. Low values of ℓ imply core penetrating character which should render the Rydberg states populated in the ZEKE experiment sensitive to decay processes, such as predissociation and rotational or vibrational auto-ionisation, arising from exchange of energy and angular momentum with the valence electrons of the positively charged cation core (see Fig. 5(a)). A contrasting

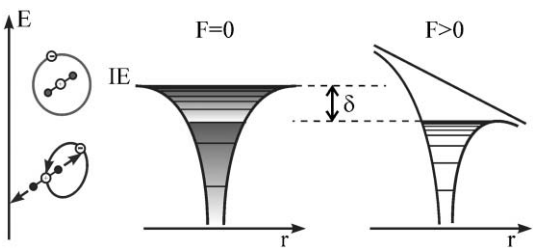

Fig. 4 A schematic representation of the field ionisation process. In the presence of an electric field, the coulomb potential (left) is modified by a linear potential, resulting in a potential (right) in which a sub-set of previously bound states become unbound. The region indicated by δ represents those Rydberg states that acquire metastable character through ℓ and m mixing. (Original diagram courtesy of K. Müller-Dethlefs.)

view emerges when one considers that from the perspective of an electron at the outer reaches of a high principal quantum number Rydberg orbit, the core will resemble a point charge, regardless of its size or structure. Intuitively, then, one expects that opportunities for very high-n Rydberg electrons to interact with the core will be far less than those of low-n Rydberg states and, in particular, of valence excited electronic states and, consequently, should have much longer lifetimes. The bottom line though, is that, even for very large Rydberg orbits, the rate of decay is directly related not only to the rate at which the electron visits the core (in a classical orbital period representation) but also to the trajectory that the electron takes which depends on its orbital angular momentum.

Low orbital angular momentum (core penetrating) Rydberg state lifetimes are proportional to the Rydberg electron density in the core region which scales as n^{-3}. Consequently, low-ℓ Rydberg states in the range n = 100–200, will have lifetimes, scaling as n^3, on the nanosecond timescale, far shorter than the typical delays imposed in typical ZEKE experiments. Given that the Rydberg states sampled in a ZEKE experiment are evidently able to survive delays well in excess of 1 μs, it becomes clear that the n^3 scaling law cannot be applied to these states. It follows that molecular Rydberg states demonstrating enhanced lifetimes must somehow have acquired non-penetrating character.

The explanation for the metastable character of the so-called ZEKE Rydberg states was first proposed by Chupka[12] who suggested that stray residual fields in the spectrometer result in Stark mixing of higher-ℓ states, reducing the penetrating character of the optically bright state and leading to a factor of n increase in lifetime (see Fig. 5(b)). In addition, inhomogeneous (time dependent) electric fields associated predominantly with ions produced from prompt ionisation, leads to m-mixing which can prolong the lifetimes by a further factor of n.[13] Strictly speaking the notion of ℓ and m mixing is an expression of the fact that neither quantum number is well defined in the presence of a stray field and that each Rydberg state is better expressed as a superposition of ℓ and m states, with states of larger values of ℓ and m making the greater contribution.

In a sense then the stray fields present in a typical apparatus are simultaneously responsible for suppressing the real zero kinetic energy electron signal yet enhancing the signal deriving from field ionisation. As a result of the early uncertainty surrounding the mechanism responsible for providing the signal, the method has variously been referred to as PFI (pulsed field ionisation), ZEKE-PFI, PFI-ZEKE, TPES, TES (threshold electron spectroscopy) as well as most commonly, and most straightforwardly, as ZEKE spectroscopy.

The ZEKE spectrum

In a typical ZEKE experiment, the appearance of the resulting spectrum depends on a number of factors, principally including the lifetime characteristics of the Rydberg states converging to each ionisation threshold, and the magnitude and make-up of the pulsed electric fields used to accomplish field ionisation. For molecules, there will be an associated Rydberg series of energy levels converging at high n to each rotational and vibrational level of the cation (see Fig. 6). Rydberg states having principal quantum numbers lower than some critical value will generally not survive the delay employed in the experiment and should not then be sampled by the field ionisation process. In practice, those states that do survive the delay (*i.e.* those states which have acquired high-ℓ and m character) have such high values of n that they form a pseudo-continuum of states, generally beyond the resolving power of the light source used. The ZEKE band associated with a particular threshold will thus have a continuous profile with a maximum intensity a few cm^{-1} below the true threshold. The shape of the band and the red-shifts in both the band onset and band maximum depend to a great extent on the field strength used. Theoretically, the red-shifts should lie between $3.1\sqrt{V}$ cm^{-1}, for *diabatic* ionisation measured at the maximum of the field ionisation band (strictly speaking, the energy at which the diabatic fall-off in the field ionisation probability begins), and $4.6\sqrt{V}$ cm^{-1}, for *diabatic* ionisation measured at the low wavenumber onset of the band.[13] In practice, the response of a ZEKE band shape to changes in electric field is not always so predictable and can be inconsistent from one experiment to

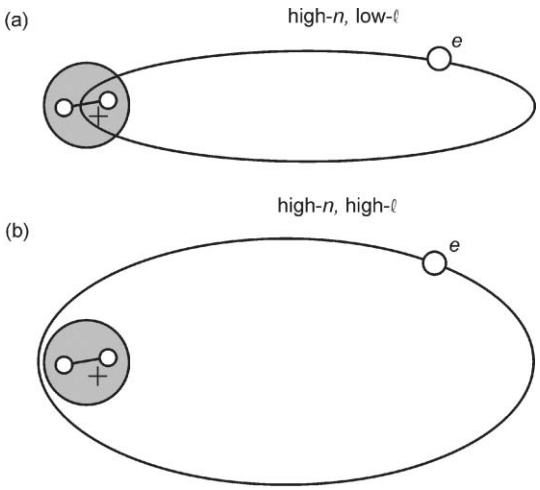

Fig. 5 A schematic representation of (a) a core-penetrating high-n Rydberg state having low-ℓ character and (b) a core-non-penetrating high-n Rydberg state of high-ℓ character.

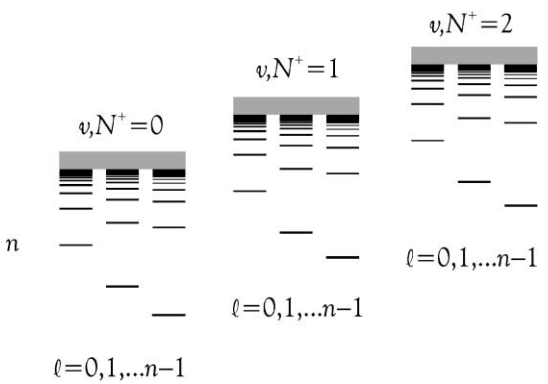

Fig. 6 An energy level diagram showing Rydberg states of different ℓ converging on three rovibrational ionisation thresholds characterised by the quantum numbers v and N^+ = 0, 1, 2.

another. Applying a blanket correction given by the theoretical response of the band to changes in field strength will not always provide a good enough account of the actual field ionisation shift and so, for many experiments, it may be necessary to extrapolate to zero field each time the experimental conditions change. Nevertheless, a reasonable generalisation would suggest that for field strengths of around 1 V cm^{-1}, we can expect the band maximum, corresponding to a principal quantum number of between 150 and 200, to be red-shifted by approximately 3 cm^{-1} with respect to the true ionisation threshold. Rydberg states of higher n values will be so sensitive to field ionisation by stray electric fields that they will have decayed by this route prior to the application of the field ionisation pulse, whilst those lying lower than $4.6\sqrt{V}$ cm^{-1}, will either not be sampled by the pulsed electric field or will have decayed *via* predissociation or auto-ionisation (for thresholds lying above the adiabatic ionisation energy).

All of these points are illustrated in Fig. 7 which shows a comparison of an optical double resonance (OODR) Rydberg spectrum of 1,4-diazabicyclo[2.2.2]-octane (DABCO) (top) with the associated ZEKE spectrum (lower, inverted).[14] Both spectra involve two-colour (1 + 1′) resonant multiphoton ionisation *via* the first excited singlet state, S_1, of DABCO. The S_1 state arises from a one-photon forbidden transition from the HOMO orbital to a 3*s* Rydberg orbital. Both spectra in Fig. 7 were recorded *via* the S_1 24^1 ($S_1{}^0$ + 1011 cm^{-1}) band and the vertical thresholds observed correspond to the 24 mode fundamental in the cation. In the OODR spectrum, which was recorded by collecting all prompt (photo)electrons under zero applied field, the second laser is scanned through the lower-*n* Rydberg series converging to the 24^1 ionisation threshold. The prompt electrons arise from auto-ionisation of the Rydberg states into the ionisation continuum lying above the vibrationless ionisation threshold. In the ZEKE experiment, the second laser scans through the very high-*n* region below the ionisation threshold ($n \geqslant 120$), with the signal deriving from pulsed field ionisation following a delay of around 1 μs.

The OODR spectrum shows a strong np_{xy} Rydberg series as well as at least two other weaker series all of which converge to the 24^1 ionisation threshold. The 24 mode series starts at $n = 11$ and extends resolvably as far as $n = 105$. The low-*n* limit is set by the location of the adiabatic ionisation threshold which lies about 40 cm^{-1} below the $n = 11$ Rydberg state. The decline in Rydberg line intensity from about $n = 50$ (decreasing to close to zero by about $n = 120$) is a reflection of the decreasing sensitivity of the Rydberg states to auto-ionisation as n increases, and the rate at which the Rydberg electron visits the core decreases. In the ZEKE spectrum, the delay before the application of the field ionisation pulse allows those Rydberg states which interact with the core to some degree to decay by auto-ionisation or predissociation, leaving just those states whose lifetimes are long enough to survive the delay. The small field strength used in the experiment samples just a small slice of Rydberg states lying within about 2 cm^{-1} of the ionisation threshold and it is these states that provide the signal. The peak in signal intensity in this case occurs for $n \approx 220$. States lying above this point generally have reduced lifetimes because of their extreme sensitivity to stray field induced decay.

Refining the technique

Once the mechanism responsible for the signal in ZEKE spectroscopy was understood, much of the subsequent development of the technique concentrated on ways to further improve the resolution. Given that the magnitude of the field strength relates directly to the depth of Rydberg states sampled by the field ionisation pulse, one obvious strategy is simply to keep the magnitude of the applied pulsed electric field to a

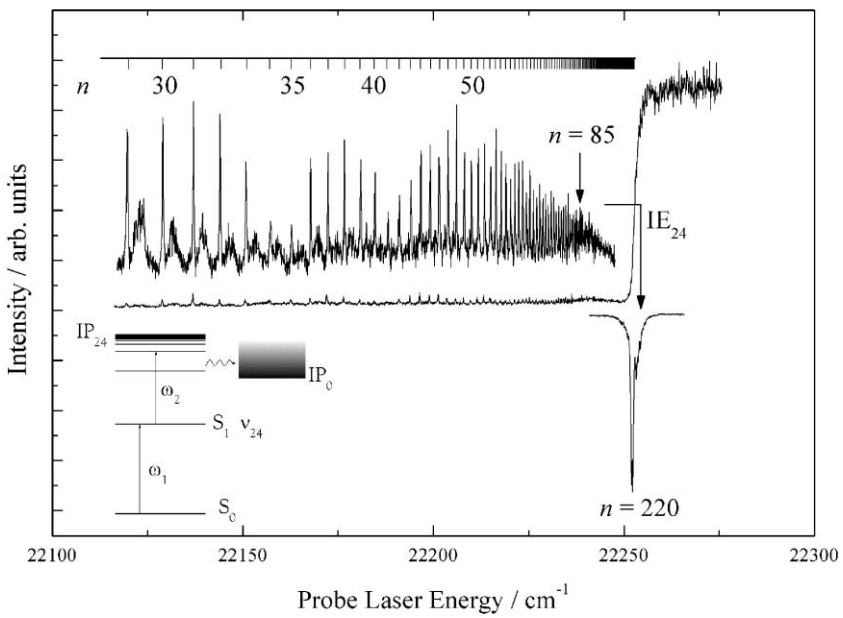

Fig. 7 A comparison of the OODR spectrum of DABCO (upper) recorded *via* the S_1 24^1 level with the ZEKE spectrum (lower, inverted) recorded *via* the same route. Note that the peak intensity in the ZEKE spectrum occurs at about $n = 220$ while the Rydberg peak intensities in the OODR spectrum have decreased to close to zero by about $n = 120$ (see text for details). [Reprinted with permission from M. J. Watkins and M. C. R. Cockett, ref. 14, Copyright 2000 American Insititute of Physics.]

minimum, albeit at a cost to signal intensity. Unfortunately, this approach, in its crudest application, is limited in practice because the very highest Rydberg states are in any case lost to stray fields and collisional ionisation. A number of alternative approaches have been used to address this problem, the most successful of which involve either sequences of pulses, or stepped or slowly rising pulses. A detailed discussion of the merits of these different approaches can be found in ref. 13, but for the purpose of this review, we shall focus briefly on the stepped pulse and the two-pulse sequence.

The main advantage of the single stepped pulse is that it allows a field dependence study of a particular ZEKE band to be conducted in a single scan. Each step in the pulse represents a small increase in field strength and by gating on the electrons produced from each step, a series of ZEKE spectra can be recorded simultaneously at a number of different field strengths (see Fig. 8). This approach requires an arbitrary function generator to design an extraction pulse with 10–30 steps, each involving a change in field strength of about 50 mV cm^{-1}. Such a pulse, illustrated in Fig. 8(a), will produce an electron time-of-flight spectrum containing as many peaks as there are steps in the pulse, and with each electron peak arising from field ionisation of a different slice of Rydberg

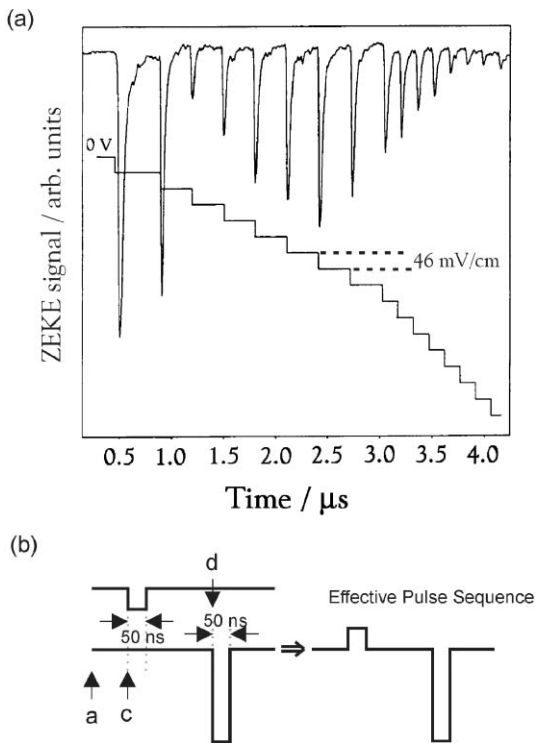

Fig. 8 (a) An illustration of a multi-stepped field ionisation pulse and the resulting electron time-of-flight pattern. Each peak in the time-of-flight spectrum corresponds to a step in the pulse. The separation of each step ranges from 480 ns at the start of the pulse to 160 ns towards the end, with each step being 46 mV cm^{-1} in height. [Reproduced (modified) with permission, I. Fischer, R. Lindner and K. Müller-Dethlefs, ref. 15.] (b) The double inverted pulse sequence, now commonly used to achieve higher resolution in ZEKE spectroscopy. The pre-pulse serves a dual purpose of removing remaining fast photoelectrons as well as top-slicing the Rydberg manifold, prior to the application of the main field ionisation pulse.

states. Setting a detection gate to each electron peak and scanning the probe laser produces a different ZEKE signal onset and band maximum corresponding to the different field strengths at each step. An extrapolation of a linear plot of signal onset against field strength yields a zeroth order ionisation threshold. The advantage of this approach in terms of outright spectral resolution over a single small square pulse is debatable but nevertheless, this method has been used to achieved a ZEKE bandwidth of 0.2 cm^{-1} in the ZEKE spectrum of benzene.[15]

The earliest applications of the two-pulse sequence were motivated initially by the need to remove prompt photoelectrons that can be trapped by a plasma of ions generated in the ionisation region of the spectrometer.[13,16] Whilst the delay employed in a ZEKE experiment will typically be sufficient to have allowed all fast photoelectrons to have left the ionisation region (or at least to have separated sufficiently for them to be discriminated against in their time-of-flight to the detector), in some instances, the high density of ions generated at the ionisation point is sufficient to trap fast photoelectrons which are then subsequently collected by the field ionisation pulse. This can lead to a high energy tail appearing on each ZEKE band.[17] One solution to this problem is to apply a pre-pulse or discrimination pulse prior to the main field ionisation pulse and usually oriented in such a way as to send the electrons in the opposite direction to the detector (see Fig. 8(b)).[16] An additional consequence of this strategy is to field ionise the top-most slice of Rydberg states which then allows the second pulse to be tuned to limit, in an entirely arbitrary way, the width of states contributing to the ZEKE signal.[18] The full potential of this approach was described in detail by Müller-Dethlefs and coworkers[19] who recognised that the first pulse in the sequence removes primarily red-shifted Stark states, leaving a remnant of blue-shifted states in the same region to be sampled by the second, opposite polarity, pulse. A consequence of the mechanism is the rather counter-intuitive observation of signal deriving from a second pulse whose magnitude is smaller than that of the first. In experiments in this laboratory, a best resolution of 0.48 cm^{-1} (FWHM) was obtained in the ZEKE spectrum of DABCO recorded using a pre-pulse of +216 mV cm^{-1} and a probe pulse of −140 mV cm^{-1}.[14] The effect of decreasing the magnitude of the probe pulse on the ZEKE band shape and position is shown in Fig. 9. In the top-most spectrum, recorded using a field strength of 1730 mV cm^{-1}, the ZEKE band appears as a broad, red-degraded Gaussian shape, with little evidence of the underlying rotational structure. As the field strength is decreased, the band shifts to higher energy, dramatically reduces in width and the underlying structure becomes more apparent. At the smallest field strength of 137 mV cm^{-1}, the separate P, Q and R branches are easily distinguished.

The best resolution in ZEKE spectroscopy has been achieved by Merkt and coworkers who obtained a resolution of better than 0.06 cm^{-1} in their spectra of argon and N_2 using a near-Fourier-transform-limited vacuum ultraviolet laser system (0.008 cm^{-1} bandwidth at 16 eV) and a variation of the double pulse ionisation scheme.[20] In their experiments the second pulse overlapped the first and consisted of a series of

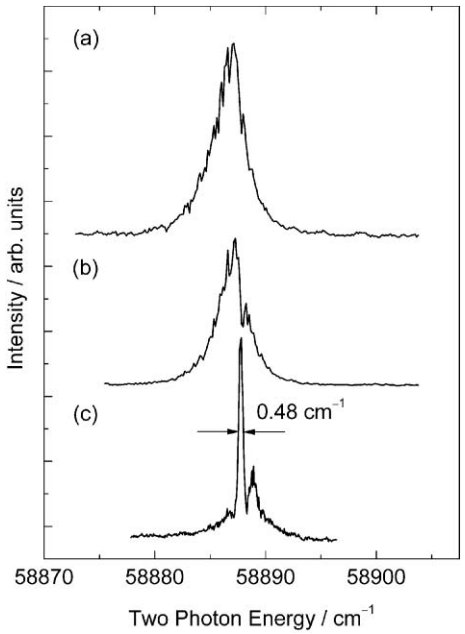

Fig. 9 The 25 mode fundamental ZEKE band of DABCO recorded at (a) 1730 mV cm^{-1}, (b) 420 mV cm^{-1} and (c) 137 mV cm^{-1}, probe pulse electric field strength. Note the effect of decreasing the magnitude of the field on the band position and bandwidth.

steps, allowing a higher selectivity of Rydberg states than is possible using a simple two pulse sequence.

Exploiting the resolution: applications

In comparison to conventional photoelectron spectroscopy, even the most run-of-the-mill ZEKE experiment will provide between one and two orders of magnitude improvement in resolution, with an additional order of magnitude available to those willing to make the effort and who have sufficient signal to play with. Applications of the technique to heavier diatomic and polyatomic molecules can therefore be expected to yield full vibrational resolution, where only electronic or partial vibrational resolution were available from PES.

For example, early HeI photoelectron spectra of I_2 show five photoelectron bands, the first two of which are associated with the two spin–orbit components of the $X^2\Pi_g$ ground electronic state of the ion, the third and fourth with the analogous spin–orbit components of the $A^2\Pi_u$ state and the fifth band with the $B^2\Sigma_g^+$ state. Fig. 10(a) shows the first three of these bands, none of which exhibit any vibrational structure at all. Ten years ago, the threshold photoelectron spectrum of I_2 was published, revealing partially resolved vibrational structure not only on the first two bands but also on the A state bands, for which the vibrational wavenumber is approximately a factor of two smaller than for the X state (Fig. 10(b)).[21] This was closely followed by a number of ZEKE studies of iodine, recorded *via* three different ionisation routes and which showed complete vibrational resolution not only of the electronic ground state but also of the first excited state.[22] The dramatic improvements in resolution between these three techniques can clearly be appreciated from the comparison of the photoelectron, threshold photoelectron and (1 + 1) ZEKE

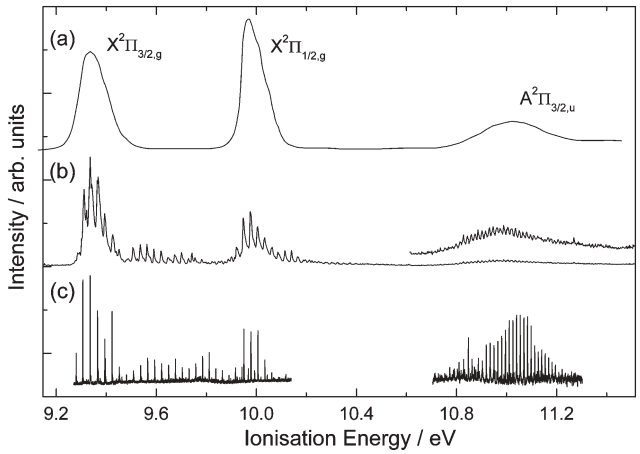

Fig. 10 A comparison of the (a) photoelectron, (b) threshold photoelectron and (c) ZEKE spectra of molecular iodine. The photoelectron and threshold photoelectron spectra were recorded using single photon direct ionisation from the electronic ground state of the neutral molecule whilst the ZEKE spectrum employed direct two-photon non-resonant ionisation. [Spectrum (b) reprinted with permission from A. J. Yencha, M .C. R. Cockett, J. G. Goode, R. J. Donovan, A. Hopkirk and G. C. King, *Threshold photoelectron spectroscopy of I_2*, p.348 (modified), ref. 21., Copyright 1994 Elsevier. Spectrum (c) reprinted with permission from M.C.R. Cockett, R.J. Donovan and K.P Lawley, ref. 22, p.3347(modified), Copyright 1996 American Institute of Physics.]

spectra of iodine shown in Fig. 10. The ZEKE spectrum reproduced in Fig. 10(c) is by no means representative of the state of the art in terms of absolute resolution, but the benefits should nevertheless be clear.

It is worth remarking on the presence of vibrational structure in regions of the ZEKE spectrum (and the TPE spectrum) of I_2 that should nominally have vanishing Franck–Condon factors (see the region between the $X^2\Pi_{3/2,g}$ and $X^2\Pi_{1/2,g}$ bands). This structure appears by virtue of a resonant auto-ionisation mechanism in which an initially excited, Franck–Condon allowed, Rydberg state (typically of low-*n*, converging to a higher threshold) couples to high-*n* Rydberg states converging to a Franck–Condon forbidden state in the cation. The end result is a population of stabilised Rydberg states that can be detected subsequently through the field ionisation process. In iodine, the vibrational progression building on the $X^2\Pi_{3/2,g}$ band origin can be followed as far as v = 90, three quarters of the way to dissociation.[22] The Franck–Condon factors for transitions directly from the neutral ground state are non-zero only for the first four or five vibrational levels.

Large amplitude motion in molecules is another example where the resolution offered by ZEKE spectroscopy can provide new information. For example, in biphenylacetylene, vibrational structure associated with the torsional motion of the two phenyl groups is clearly observed in the ZEKE spectrum.[23] In that study, ZEKE spectra were recorded *via* the zero point level as well as the first two even quanta torsional levels in the $S_1(^1B_{1u})$ state. Whilst the REMPI spectra show intensity only in even quanta torsion levels, both odd and even quanta levels appear in the ZEKE spectra, suggesting a

vibronic coupling mechanism to a higher lying cation electronic state. A fit of the vibrational term values to a two-fold potential yielded a barrier to internal rotation approximately ten times larger than that of the neutral electronic ground state. The assumption made in that work that the potential barrier to torsional motion is related directly to the degree of electron conjugation suggests that ionisation greatly increases electron conjugation between the acetylene and phenyl group π electrons.

ZEKE spectroscopy is not limited to the electronic ground state of the ion. Core excited ZEKE Rydberg states exhibit much the same metastable character as those associated with the electronic ground state and allow acquisition of ZEKE spectra of electronically excited states. In fact, these Rydberg states are so robust that the core can undergo any number of decay processes, with the Rydberg electron essentially unaware of any structural or electronic changes to the core. A particularly dramatic example of this is provided by the ZEKE spectrum of the $A^2\Sigma$ state of HBr^+.[24] For the v = 0 and 1 levels the ion is stable, having a fluorescence lifetime of the order of microseconds. However, the v = 2 and v = 3 levels are predissociated, having lifetimes of 10^{-10} and 10^{-13} s, respectively, and yet ZEKE spectra of both bands were recorded successfully. This implies that the ZEKE Rydberg electron is essentially unperturbed by the dissociation of the core, and continues orbiting the Br^+ fragment after the departure of the H atom.

A more recent example of electronically excited ZEKE spectroscopy is provided by the ZEKE spectrum of the $\tilde{A}^2\Pi$ state of OCS^+. OCS (as well as CO_2 and CS_2) provide an opportunity to study the Renner–Teller effect in molecules subject to both spin–orbit coupling and Fermi resonances. Sommavilla and Merkt[25] used coherent VUV radiation generated by two-photon resonance-enhanced sum-frequency mixing in krypton to excite direct one-photon transitions to the excited state of the ion from the neutral ground state. All of the vibrationally excited levels of the A state of the ion are predissociated, with natural line widths larger than the rotational spacing and so this particular study concentrated on an analysis of the vibrational structure. The ZEKE spectrum of the $\tilde{A}$ state band is shown in Fig. 11. The spectrum covers over 7000 cm^{-1} and is made up of a series of vibrational progressions involving combinations of the CS and CO stretching modes (ν_1 and ν_3, respectively), split by spin–orbit coupling so that transitions to each vibration appear as doublets separated by about 120 cm^{-1}. In addition, the higher members of the ν_1 progressions where $\nu_1 \geqslant 1$ are further split by Fermi resonances with the bending mode levels. In linear molecules such as OCS^+, a doubly degenerate Π state may lose its degeneracy when the bending mode is excited. This effect is known as the Renner–Teller effect and in the ZEKE spectrum of the $\tilde{A}$ state of OCS^+ results in additional splittings and perturbations to the already complex vibrational structure. Although excitation of the bending mode directly in the $\tilde{A}$ state is very weak for transitions from the electronic ground state of the neutral molecule, these transitions gain intensity from a coupling between the CS stretching levels and the bending mode levels through the Fermi resonances. The vibrational analysis published in ref. 25 allowed a revision of

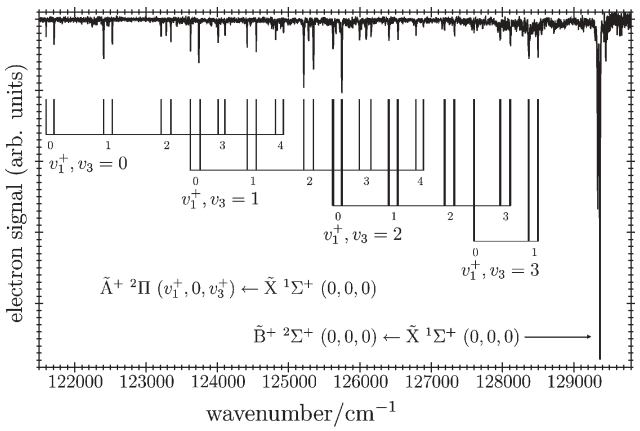

Fig. 11 ZEKE spectrum of OCS in the region of the $\tilde{X}\,^1\Sigma^+ \rightarrow \tilde{A}^+\,^2\Pi$ and $\tilde{X}\,^1\Sigma^+ \rightarrow \tilde{B}^+\,^2\Sigma^+$ bands. The assignment bars indicate four vibrational progressions in the CS stretching mode (ν_1), appearing in combination with up to three quanta in the CO stretching mode (ν_3). Each vibrational band appears as a spin–orbit split doublet. For higher members of the progression, Fermi resonances lead to additional fine structure. [Reprinted with permission from ref. 25. Copyright 2004 American Chemical Society.]

the bending mode wavenumber downwards by over 40 cm^{-1} to $<$360 cm^{-1} from that published previously.

Fluorobenzene is an example of a molecule whose photoelectron spectrum reveals essentially no vibrational structure but whose ZEKE spectrum is not only fully vibrationally resolved but can also reveal partial rotational resolution. In a very recent study of fluorobenzene and the fluorobenzene–Ar van der Waals complex, Ford and Müller-Dethlefs[26] obtained partial rotational resolution using a novel ZEKE electron detection scheme to record ZEKE *excitation* spectra obtained by scanning the pump laser in a two-colour (1 + 1′) excitation scheme whilst keeping the ionising laser wavelength fixed. A ZEKE excitation spectrum is effectively one dimension of a two-dimensional spectrum because the ZEKE signal depends on the energy of both the pump and probe lasers: the excitation laser determines which subset of rotational levels is populated prior to the ionisation step, whilst the ionisation laser excites the transition between rotational levels in the neutral excited intermediate state and those in the cation ground state. The end result is an excitation spectrum that displays more rotational detail than would otherwise be observable in the other dimension, *i.e.* that seen in the conventional ZEKE spectrum. Fig. 12 shows comparisons between experimental and simulated ZEKE excitation spectra, recorded by fixing the ionisation laser at various rotational transitions into the origin band of the cation and scanning the pump laser wavelength. The simulated fits of the observed spectra, using a spectator orbital model, allowed rotational constants for both the fluorobenzene and fluorobenzene–Ar cations to be obtained for the first time.

Rotationally resolved ZEKE spectra have the potential to provide the greatest insights into the structure of molecular ions. However, the heavier and larger the molecule the smaller the rotational constants and the more technically challenging the experiment. Nevertheless, with the potential for such high spectral resolution, ZEKE spectroscopy can and has been used

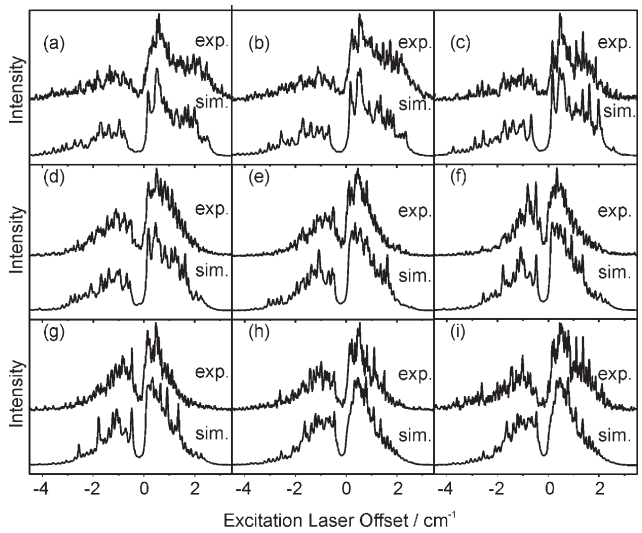

Fig. 12 Experimental (top) and simulated (bottom) ZEKE excitation spectra of fluorobenzene, with the ionisation laser fixed at various rotational transitions into the origin band of the cation. [M. S. Ford and K. Müller-Dethlefs, ref. 26. Reproduced by permission of the PCCP owner societies.]

in a number of studies to obtain fully rotationally resolved spectra. For example, Merkt and coworkers have recently obtained the first rotationally resolved spectra of the methane cation using ZEKE spectroscopy.[27] The ground state of the tetrahedral methane cation is doubly degenerate and as a result is potentially subject to the Jahn–Teller effect. Merkt studied a number of different isotopomers of CH_4^+ and found that, for all except $CH_2D_2^+$, the Jahn–Teller effect is so small that each cation undergoes simple pseudo-rotational tunnelling motion between numerous equivalent minima (six in CH_4/CD_4 and three in CH_3D). However, $CH_2D_2^+$ behaves as a rigid rotor, exhibiting the static Jahn–Teller effect with its structure frozen into one of the C_{2v} minima.

Perhaps the benchmark example of how rotational resolution has helped to resolve a classic structural question is benzene, one of the largest molecules exhibiting fully rotationally resolved ZEKE spectra. Benzene$^+$, in common with methane$^+$, is subject to the Jahn–Teller effect because its electronic ground state is doubly degenerate. According to *ab initio* theory, in-plane distorted geometries with elongated or compressed D_{2h} structures should be more stable than the higher symmetry D_{6h} geometry. If the molecule were distorted to lower symmetry, transitions should appear in the rotationally resolved ZEKE spectrum that would be forbidden in the D_{6h} structure. Fig. 13 shows the rotationally resolved ZEKE spectrum of the 6^1 ($j = \pm\frac{3}{2}$) band of benzene$^+$ recorded *via* the rovibronic state $S_1 6^1$ ($J' = 2$, $K' = 2. - \ell$).[15] The analysis of this spectrum allows assignment of the lower energy component, displaying transitions to even N^+ levels for $K^+ = 0$, to B_{1g} vibronic symmetry and the higher energy component, which displays transitions to odd N^+ levels for $K^+ = 0$, to B_{2g} vibronic symmetry. One of the most important conclusions drawn from this analysis is that benzene has D_{6h} symmetry both in the neutral intermediate state as well as in the electronic ground state of the cation rather than the theoretically more stable D_{2h} structures.

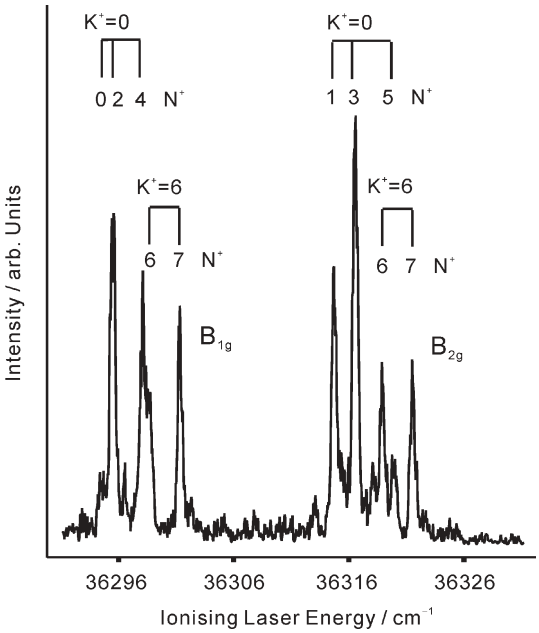

Fig. 13 The rotationally resolved ZEKE spectrum of the 6^1 ($j = \pm\frac{3}{2}$) band of benzene$^+$ recorded *via* the rovibronic state $S_1 6^1$ ($J' = 2$, $K' = 2. - \ell$). The analysis of this spectrum allows assignment of the lower energy component, displaying transitions to even N^+ levels for $K^+ = 0$, to B_{1g} vibronic symmetry and the higher energy component, which displays transitions to odd N^+ levels for $K^+ = 0$, to B_{2g} vibronic symmetry. [Reprinted with permission from K. Müller-Dethlefs, *Applications of ZEKE Spectroscopy*, ref. 46. Copyright 1995 Elsevier.]

A large number of studies of molecular van der Waals complexes have been made in the past 15 years or so using ZEKE spectroscopy, none of which could have been accomplished using conventional PES.[28] The very weak nature of the van der Waals interaction implies intermolecular vibrational wavenumbers in the range 5 to 50 cm^{-1}. Virtually all ZEKE studies of van der Waals molecules have been made using two-colour ionisation schemes because of the obvious advantages that this route offers in terms of state selectivity and molecule specificity. Many of these studies have focused on aromatic molecules with solvents ranging from rare gas atoms to a wide variety of polar and non-polar molecular solvents. Recently there has been some attention paid to interactions involving molecules of biological relevance where solvation can potentially provide insight into the ways that biomolecules respond to their environment. For example, Ullrich *et al.*[29] have made a recent study of the *trans*-formanilide–H_2O complex using two-colour REMPI and ZEKE spectroscopy. Formanilide exists either as a *trans* or *cis* isomer in the gas phase, but only the *trans* form of the water complex has been observed spectroscopically. In the gas phase, the water molecule can bind to the N–H group, in which case it acts as a proton acceptor, or to the C=O group, where it acts as a proton donor. In the REMPI spectrum, the band origins of the NH and CO bound complexes are shifted by -218 cm^{-1} and $+118$ cm^{-1}, respectively, with respect to the formanilide band origin, representing the relative strengths of the hydrogen bonding in the S_1 state relative to the electronic ground state. The ZEKE spectra recorded *via* the NH isomer band origin and a number

of inter- and intramolecular vibrational intermediate levels reveal rich intermolecular vibrational structure together with an ionisation energy red-shift of nearly 3800 cm^{-1} (see Fig. 14). In the spectrum recorded *via* the band origin, the dominant band at 0 cm^{-1} ion internal energy corresponds to the transition to the zero point level in the cation, with the weaker vibrational structure appearing to higher energy due to excitation of van der Waals vibrational modes. A characteristic of this type of pump-probe study is that, as the level of vibrational excitation is increased in the intermediate state, so the intensity shifts to higher energy in the respective ZEKE spectra. In other words, exciting the molecule prior to ionisation results in a preferentially vibrationally excited cation. Interestingly, the ZEKE spectrum recorded for the CO bound complex shows the same ionisation energy shift as the NH isomer, suggesting that the CO isomer converts to the NH form upon ionisation.

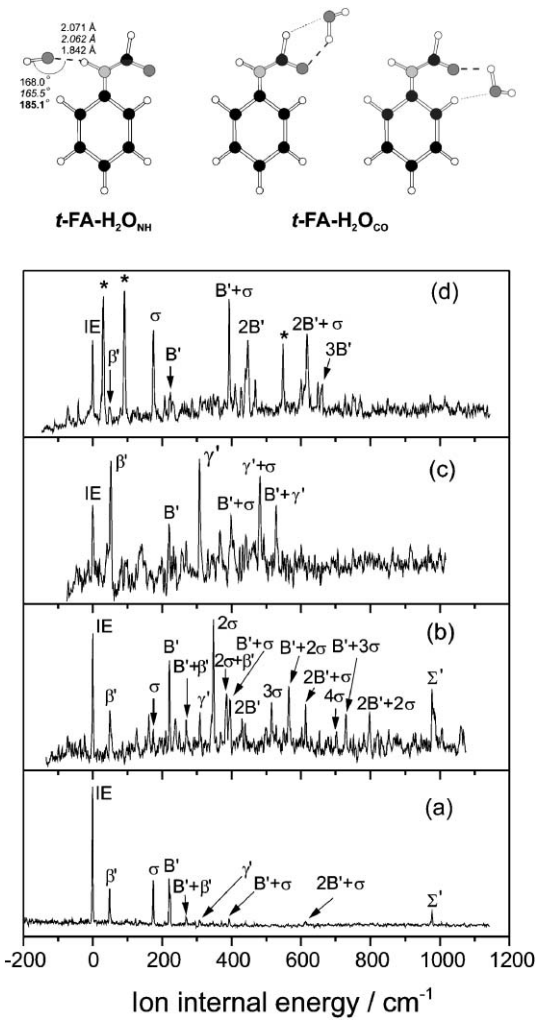

Fig. 14 ZEKE spectra of *t*-FA-H_2O_{NH} recorded *via* the (a) S_1 0^0, (b) S_1 σ (intermolecular stretch), (c) S_1 γ′ (intermolecular in-plane wag) and (d) S_1 B′ (intermolecular in-plane bend). Calculated structures (CASSCF/cc-pVDZ) of the *t*-FA-H_2O_{NH} and *t*-FA-H_2O_{CO} structures are displayed at the top of the figure. [S. Ullrich, X. Tong, G. Tarcsay, C. E. H. Dessent and K. Müller-Dethlefs, ref. 29. Reproduced by permission of the PCCP owner societies.]

ZEKE spectroscopy has also been applied successfully to a number of metal containing species. These range from small metal clusters, to metal atom complexes, metal oxides and organometallic species.[30] A recent example of an organometallic species is the Cu–ethylenediamine complex, produced by the reaction of laser vaporised copper atoms with ethylenediamine vapour.[31] Ethylenediamine is widely used as a chelating ligand in inorganic chemistry and in the gas phase, the most stable rotational isomers are predicted to have *gauche* configurations with an intramolecular H–N···H hydrogen bond. Four possible isomers are predicted for the copper complex, illustrated in Fig. 15 (top). These comprise two H-bonded structures, differentiated by the Cu–N–C–C dihedral angle, a ring structure formed with the Cu atom bound to both N atoms and a *trans* structure formed by the Cu binding to one nitrogen of the *trans* conformer. The ZEKE spectrum of the molecule was recorded *via* a single photon ionisation scheme employing the frequency doubled output of an excimer

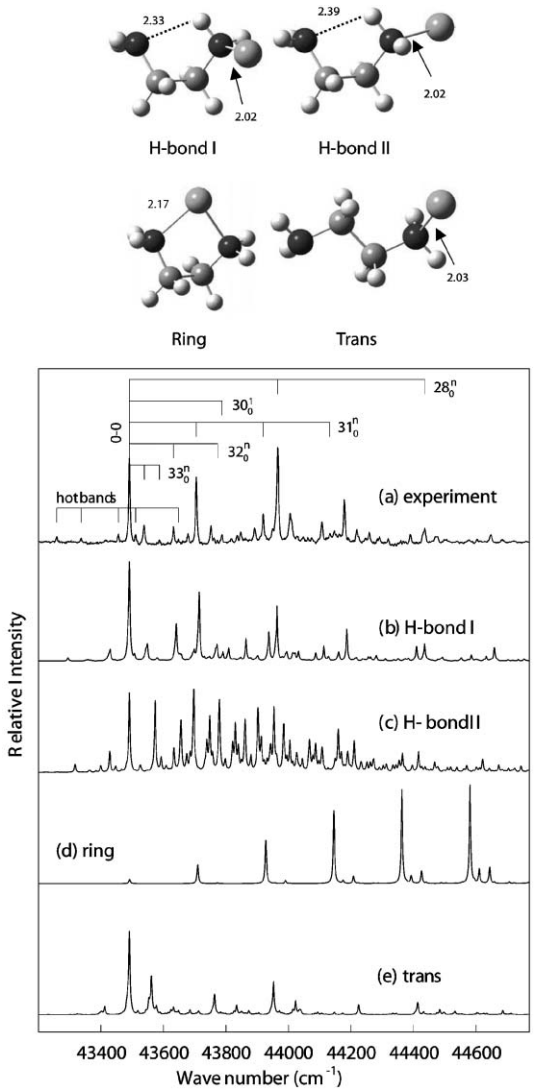

Fig. 15 The ZEKE spectrum of the Cu–ethylenediamine complex seeded in Ar (a) and simulations (80 K) of four isomers (b)–(e) (shown at the top of the figure). [Reprinted (modified) with permission from ref. 31. Copyright 2004 American Chemical Society].

pumped dye laser. The spectrum is rich in vibrational structure with progressions in the Cu–N stretch, Cu–N–C bend, Cu–N–C–C torsion, H-bond stretch and NH_2 rock modes. Comparisons of the experimental spectrum with simulated spectra for the four isomers allows an assignment to the H-bond I structure (See Fig. 15(a)), indicating that the overall stabilisation of the N···H and Cu–N bonds is larger than the two Cu–N bonds in a bidentate structure. This contrasts with the potassium complex which had been found to form a ring structure. This difference arises from a larger electron repulsion between the metal 4s electron and the nitrogen lone pair orbital in copper than in potassium.

Variations on a theme

The great appeal of the ZEKE method is its potential for exceptional resolution, its robustness in terms of the type of systems that can be studied and the relative ease with which a standard REMPI or time-of-flight photoelectron apparatus can be modified to work as a ZEKE spectrometer. In constructing a ZEKE apparatus, some care is required to shield the ionisation region from stray magnetic and electric fields, usually through the use of mu metal shielding, but even this is not strictly necessary to get workmanlike quality spectra.

Ionisation schemes employing single photon coherent VUV[24] or XUV[32] sources, resonant multiphoton two-colour (1 + 1′),[33] (2 + 1′)[34], (3 + 1′),[35] (1 + 2′),[36] one-colour two-photon non-resonant (1 + 1)[22] ionisation as well as ionisation using synchrotron sources[37] have all been used successfully to study a wide range of atoms, molecules, radicals, metals, biomolecules and numerous atomic and molecular van der Waals complexes and clusters. Probably the most common ionisation schemes employ two-colour resonant ionisation for the experimental convenience, the state selectivity it offers and the prospect for manipulation of Franck–Condon factors to probe regions of the ionic state potential surface not necessarily accessible directly from the neutral ground state. Anions have also been studied using the technique but as they do not possess Rydberg states the method reverts to true threshold ionisation involving detection of threshold photo-electrons.[38] In contrast to ZEKE spectroscopy of the neutral, which yields information on the corresponding cation, anion ZEKE provides information on the neutral molecule. The experimental challenges involved are considerably more arduous, however, as a very great deal more care has to be taken to ensure that stray fields are kept to an absolute minimum.

One of the perceived shortcomings of the method as originally conceived was the difficulty in unambiguously associating the signal with a particular species. Two-colour ZEKE has the advantage in this respect over direct one-photon ionisation schemes in that state selection imparts a substantial degree of molecule specificity, particularly important in studies of molecular clusters. However, there is still the possibility that overlapping transitions at the intermediate level in a pump-probe experiment can give rise to signals from other species in the system. An obvious strategy to overcome this problem is simply to detect the *ions* produced from the field ionisation mechanism rather than the electrons. In principle this then allows all of the advantages of high resolution and state selectivity in two colour experiments but with the added bonus of mass selectivity and therefore molecule specificity. In 1991, Zhu and Johnson developed a technique for separating slow photo-ions from high-*n* Rydberg states, thereby enabling the measurement of so-called mass-analysed threshold ionisation (MATI) spectra.[39] The main technical challenge derives from the fact that prompt photo-ions are very much heavier and therefore slower than electrons and as a consequence are rather more difficult to distinguish from ions generated by field ionisation of high-*n* Rydberg states. The solution requires the initial laser excitation to be carried out upstream in the molecular beam, allowing sufficient time to pass for a small electric field to separate the photo-ions from the surviving neutral Rydberg states. This process usually requires a delay of up to 10 microseconds or more between the laser shot and the subsequent application of a high voltage pulse, used to field ionise the Rydberg states. High voltage is needed for the final step because the ions need to be accelerated into the time-of-flight detector. The original MATI technique works very well, but in general provides spectra of rather lower resolution than ZEKE spectra because of the large electric fields required for the field ionisation step. However, this problem can be resolved by using a modification of the double pulse technique used in ZEKE spectroscopy to obtain spectra of comparable resolution to ZEKE spectroscopy.[40] Numerous examples of the application of MATI spectroscopy can be found in the literature, covering similar ground to that covered by ZEKE spectroscopy. However, one of the particularly attractive features of MATI spectroscopy is the ability to monitor the onset of dissociation in an ion by monitoring the daughter ion mass channels. Braun and Neusser, for example, were able to monitor the appearance of benzene cations from the MATI spectrum of benzene–Ar, thereby obtaining an accurate measure of the dissociation energy of the complex.[41]

The same group adopted a very novel approach to obtaining very high resolution spectra of benzene–rare gas complexes by exploiting the inherent breadth of the MATI signal in a variation of the MATI method.[42] In their experiments, they used two single mode CW ring dye lasers to promote two-colour resonant excitation to Rydberg states converging to various rovibronic thresholds of the ion. The magnitude of the field ionisation pulse was such that single *n* Rydberg states could be resolved from about $n = 45$ to 110 for the benzene–Ar complex. The novelty of their approach lay in an automated cross-correlation of the measured Rydberg series with a simulated series to obtain the so-called cross-correlation ionisation energy spectrum (CRIES). This procedure revealed the different Rydberg series limits associated with different rotational states of the ion (see Fig. 16).

A similar experiment conducted in this laboratory,[43] investigated whether the additional complexity of a *molecular* solvent bound to a polyatomic molecule allows equally well-resolved high-*n* Rydberg structure and whether that structure shows any evidence of perturbations due to interactions between the degrees of freedom of the core and the Rydberg electron. Fig. 17 shows a comparison of the two-colour (1 + 1′) MATI and ZEKE spectra of the van der Waals complex,

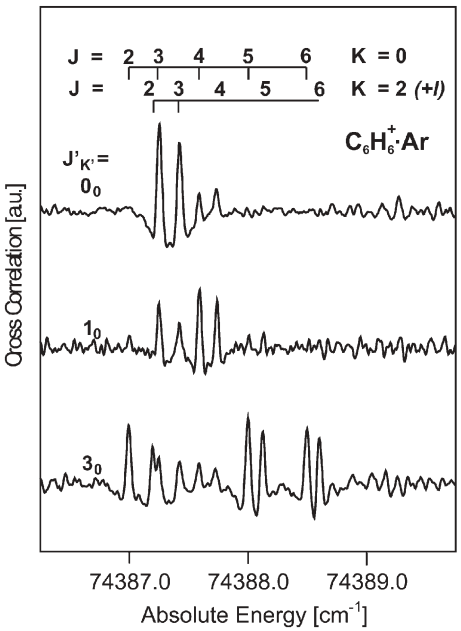

Fig. 16 Cross-correlation ionisation energy spectra (CRIES) representing the Rydberg series limits of C_6H_6·Ar measured *via* S_1 6^1 intermediate states with $K' = 0$ and three different J' values. Transitions into two J-stacks with $K = 0$ and $K = 2$, $(+\ell)$ are observed. [Reprinted with permission from Klaus Siglow, ref. 42. Copyright 1999 American Institute of Physics.]

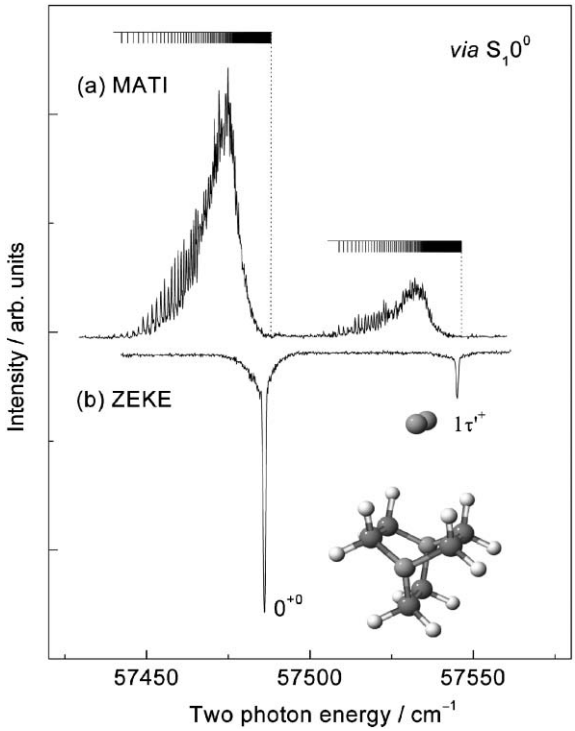

Fig. 17 A comparison of the two-colour (1 + 1′) MATI spectrum of DABCO-N_2 recorded *via* the $S_1 0^0$ band origin with the analogous ZEKE spectrum. Each spectrum shows two bands, the first corresponding to the cation band origin ($v = 0$) and the second to the van der Waals mode fundamental (labelled $1\tau'^+$). Each band in the MATI spectrum consists of a single resolved Rydberg series extending from $n = 49$ for the band origin and $n = 54$ for the $1\tau'^+$ band. [Reproduced with permission from ref. 43. Copyright 2004 American Physical Society].

DABCO–N_2, recorded *via* the first singlet excited state band origin ($S_1 0^0$). The two spectra are essentially equivalent to each other, exhibiting course vibrational structure characteristic of the electronic ground state of the complex cation. The first, and most intense band in each spectrum is assigned to the band origin and the second, weaker band which lies 59 cm^{-1} to higher energy, is assigned to one quantum excited in a van der Waals mode, labelled $1\tau'^+$. The widely different field strengths used in the two experiments result in dramatically different band widths: At the field strengths used in the ZEKE spectrum, field ionisation onset occurs at around $n = 160$, with a maximum in ionisation cross-section occurring around $n = 185$ and then declining to zero at about $n = 205$. The resulting ZEKE bandwidth in this case is of the order of 1 cm^{-1} (FWHM) and allows resolution of the underlying rotational branch structure. The much higher field strengths employed in the MATI experiment sample states lying within 50 cm^{-1} of each threshold, extending down to about $n = 50$. As a result the MATI spectra have a band width of about 15 cm^{-1} (FWHM), but more interestingly show the finely resolved substructure of the Rydberg series converging to a given ionisation threshold. A high resolution scan of the $1\tau'^+$ band recorded *via* the $S_1 1\tau'$ intermediate state is shown in Fig. 18. The spectrum shows a single Rydberg series with an onset at about $n = 58$ and is resolvable as far as $n = 96$. The fact that any signal is seen at all implies that all of the resolved Rydberg states have lifetimes exceeding the 10 μs delay employed after the laser shot. Although the line positions of the Rydberg series are largely unperturbed (within the limits of the spectral resolution), it is noticeable that the intensity does fluctuate somewhat, with a number of negative dips in intensity observable throughout the spectrum. The most likely explanation for this is the presence of lower-n ($33 \leqslant n \leqslant 39$) core-excited Rydberg states in this region, converging to the

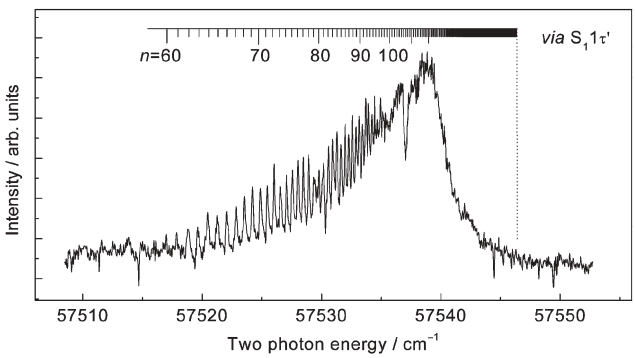

Fig. 18 A high resolution scan of the $1\tau'^+$ MATI band recorded *via* the $S_1 1\tau'$ intermediate state. The spectrum shows a single Rydberg series with an onset at about $n = 58$ and resolvable as far as $n = 96$. The lower separation field used in this case has resulted in a very well resolved Rydberg series extending over a much larger range of principal quantum number than in the other MATI spectra (which start lower but do not extend to such high values of n). [Reproduced with permission from ref. 43. Copyright 2004 American Physical Society.]

$2\tau'^{+}$ band: the loss of intensity at these positions is due to a mixing of the much shorter lifetime $2\tau'^{+}$ Rydberg states with the metastable $1\tau'^{+}$ states, which then do not survive the 10 μs delay. The key question arising from this result is whether or not it is reasonable to expect the orbiting Rydberg electron to be perturbed by or interact with the rotating and vibrating ionic core. Rotation of the charge centre about the centre of mass resembles a rotating dipole with a dipole moment considerably larger than that of neutral polar molecules. Similarly, excitation of a van der Waals intermolecular mode leads to a periodically changing dipole oscillating on a timescale somewhat shorter than rotation. However, the observation of essentially unperturbed Rydberg series suggests that even for large polar molecular cores bound by a complex mixture of dispersion, charge and quadrupole–quadrupole interactions, the classical orbital periods of Rydberg electrons in the range $n = 60$ to 100 are sufficiently different to the rotational or vibrational periods of the core for there to be negligible interaction.

One further spectroscopic development, known as Photoinduced Rydberg Ionisation (PIRI), is also worthy of mention, in spite of the fact that it has not been so widely adopted as ZEKE and MATI spectroscopies. This method was also developed by Johnson and coworkers,[44] and uses a double resonance technique to create electronically core excited Rydberg states *via* Rydberg state intermediates converging to the lowest ionisation limit. Subsequent auto-ionisation leads to signal which allows spectroscopic characterisation of electronically excited states of the ion. There are still some question marks over the mechanism by which the method works, but it nonetheless offers a highly sensitive approach for direct spectroscopy of the cation as well as a means to conducting spectroscopy on state selected ions.

Prospects for the future

ZEKE spectroscopy is now a mature technique, having spawned numerous methodological offshoots and having been applied to an extremely diverse range of problems. It has been adopted world wide and has become one of the default methods of choice for high resolution spectroscopy of the ion. Applications of pulsed field ionisation methods can generally be divided into those that are concerned with the benefits offered by the inherent sensitivity and high resolution of spectroscopic methods such as ZEKE and MATI spectroscopy and those that focus on understanding Rydberg dynamics and in manipulating and applying the properties of Rydberg states to particular problems. Many of the applications in the latter category, such as Rydberg tagging of molecular photofragments, the control of translational and orientational motion using the Stark effect on Rydberg states, and the study of reactive collisions of Rydberg molecules in the gas phase and at surfaces, are still in their infancy.[45] However, these areas provide a glimpse of the ways in which this aspect of the subject may develop in the future.

The recent growth in the number of synchrotron studies employing multibunch mode operation[37] potentially offers the prospect of high resolution XUV studies of highly excited electronic states of the cation. MATI spectroscopy provides an ideal way of preparing ions in well defined internal states for subsequent reaction. Indeed, some time ago, Mackenzie *et al.* used pulsed field ionisation methods to study reactive scattering of state-selection H_2^+ ions with neutral H_2 in the reaction $H_2^+ + H_2 \rightarrow H_3^+ + H$.[45] A handful of subsequent studies of other reactions have been made, some of which show vibrational state dependence of product ion yield but none of which show any dependence on the ionic *rotational* energy state.[45] One can envisage similar studies being made using molecular complexes to prepare a state-selected half-collision complexes for ion–molecule chemistry. In general, though, the spectroscopy of the ion is under explored compared to the neutral state and the potential scope for future applications of ZEKE spectroscopy seems limited only by the imagination of those who choose to use it.

References

1 See for example K. Müller-Dethlefs, M. Sander and E. W. Schlag, *Chem. Phys. Lett.*, 1984, **112**, 291.
2 M. I. Al-Joboury and D. W. Turner, *J. Chem. Soc.*, 1963, 5141.
3 F. I. Vilesov, B. C. Kurbatov and A. N. Terenin, *Dokl. Akad. Nauk SSSR*, 1961, **138**, 1329.
4 R. S. Mulliken, *Phys. Rev.*, 1948, **74**, 736.
5 T. Koopmans, *Physica*, 1934, **1**, 104.
6 A. M. Rijs, E. H. G. Backus, C. A. de Lange, N. P. C. Westwood and M. H. M. Janssen, *J. Electron Spectrosc. Relat. Phenom.*, 2000, **112**, 151.
7 R. Weinkauf, F. Lehrer, E. W. Schlag and A. Metsala, *Faraday Discuss.*, 2000, **115**, 363.
8 D. Villarejo, *J. Chem. Phys.*, 1968, **48**, 4014.
9 W. B. Peatman, T. B. Borne and E. W. Schlag, *Chem. Phys. Lett.*, 1969, **3**, 492.
10 G. C. King, A. J. Yencha and M. C. A. Lopes, *J. Electron Spectrosc. Relat. Phenom.*, 2001, **114**, 33.
11 G. Reiser, W. Habernicht, K. Müller-Dethlefs and E. W. Schlag, *Chem. Phys. Lett.*, 1988, **152**, 119.
12 W. A. Chupka, *J. Chem. Phys.*, 1993, **98**, 4520.
13 F. Merkt, *Annu. Rev. Phys. Chem.*, 1997, **48**, 675 and references therein.
14 M. J. Watkins and M. C. R. Cockett, *J. Chem. Phys.*, 2000, **113**, 10560.
15 I. Fischer, R. Lindner and K. Müller-Dethlefs, *J. Chem. Soc., Faraday Trans*, 1994, **90**, 2425.
16 M. C. R. Cockett, K. Okuyama and K. Kimura, *J. Chem. Phys.*, 1992, **97**, 4679.
17 See for example the ZEKE spectra of *m*-chlorophenol in: M. C. R. Cockett, M. Takahashi, K. Okuyama and K. Kimura, *Chem. Phys. Lett.*, 1991, **187**, 250.
18 M. C. R. Cockett and K. Kimura, *J. Chem. Phys.*, 1994, **100**, 3429.
19 H. J. Dietrich, K. Müller-Dethlefs and L. Y. Baranov, *Phys. Rev. Lett.*, 1996, **76**, 3530.
20 U. Hollenstein, R. Seiler, H. Schmutz, M. Andrist and F. Merkt, *J. Chem. Phys.*, 2001, **115**, 5461.
21 A. J. Yencha, M. C. R. Cockett, J. G. Goode, R. J. Donovan, A. Hopkirk and G. C. King, *Chem. Phys. Lett.*, 1994, **229**, 347.
22 M. C. R. Cockett, R. J. Donovan and K. P. Lawley, *J. Chem. Phys.*, 1996, **105**, 3347 and references therein.
23 K. Okuyama, M. C. R. Cockett and K. Kimura, *J. Chem. Phys.*, 1992, **97**, 1649.
24 J. W. Hepburn, *Chem. Soc. Rev.*, 1996, **25**, 281 and references therein.
25 M. Sommavilla and F. Merkt, *J. Phys. Chem. A*, 2004, **108**, 9970.
26 M. S. Ford and K. Müller-Dethlefs, *Phys. Chem. Chem. Phys.*, 2004, **6**, 23.
27 R. Signorell and F. Merkt, *Faraday Discuss.*, 2000, **115**, 205.
28 C. E. H. Dessent and K. Müller-Dethlefs, *Chem. Rev.*, 2000, **100**, 3999 and references therein.
29 S. Ullrich, X. Tong, G. Tarcsay, C. E. H. Dessent and K. Müller-Dethlefs, *Phys. Chem. Chem. Phys.*, 2002, **4**, 2897.

30 D-S. Yang and P. A. Hackett, *J. Electron Spectrosc. Relat. Phenom.*, 2000, **106**, 153 and references therein.
31 X. Wang and D.-S. Yang, *J. Phys. Chem. A.*, 2004, **108**, 6449.
32 W. Kong and J. W. Hepburn, *Can. J. Phys.*, 1994, **72**, 1284.
33 See numerous examples cited in, for example, M. C. R. Cockett, K. Müller-Dethlefs and T. G. Wright, *Annu. Rep. Prog. Chem. C.*, 1998, **94**, 327; R. C. Shiell and T. G. Wright, *Annu. Rep. Prog. Chem. C.*, 2002, **98**, 375.
34 M. C. R. Cockett, *J. Electron Spectrosc. Relat. Phenom.*, 1998, **97**, 171.
35 T. K. Ha, P. Rupper, A. Wuest and F. Merkt, *Mol. Phys.*, 2003, **101**, 827.
36 M. C. R. Cockett, *J. Phys. Chem.*, 1995, **99**, 16228.
37 C. Y. Ng, *Ann. Rev. Phys. Chem.*, 2002, **53**, 101.
38 V. Distelrath and U. Boesl, *Farad. Discuss.*, 2000, **115**, 161 and references therein.
39 L. Zhu and P. M. Johnson, *J. Chem. Phys.*, 1991, **94**, 5769.
40 C. E. H. Dessent, S. R. Haines and K. Müller-Dethlefs, *Chem. Phys. Lett.*, 1999, **315**, 103.
41 J. E. Braun and H. J. Neusser, *Mass. Spectrom. Rev.*, 2002, **21**, 16.
42 K. Siglow, R. Neuhauser and H. J. Neusser, *J. Chem. Phys.*, 1999, **110**, 5589.
43 M. C. R. Cockett and M. J. Watkins, *Phys. Rev. Lett.*, 2004, **92**, 43001.
44 D. P. Taylor, J. G. Goode, J. E. Leclaire and P. M. Johnson, *J. Chem. Phys.*, 1995, **103**, 6293.
45 T. P. Softley, *Int. Rev. Phys. Chem.*, 2004, **23**, 1 and references therein.
46 K. Müller-Dethlefs, *J. Electron Spectrosc. Relat. Phenom.*, 1995, **75**, 37.

